

Effect of geometry on the time law of Liesegang patterning

István Lagzi^a, András Volford^{b,*}, András Büki^c

^a Department of Physical Chemistry, Eötvös University, P.O. Box 32, Budapest H-1518, Hungary

^b Department of Chemical Physics, Budapest University of Technology and Economics, Budapest H-1521, Hungary

^c In Silico Ltd., Nagyszombat s. 25., Budapest H-1034, Hungary

Received 12 July 2004; in final form 3 August 2004

Abstract

Evolution of Liesegang patterns in 2D radially symmetric gel media was studied experimentally in the $\text{AgNO}_3/\text{K}_2\text{Cr}_2\text{O}_7/\text{gelatine}$ system. Different initial conditions were applied by varying the radius of the hole from which the penetration of the invading electrolyte took place. Our results show that the characteristics of the final pattern weakly depend on this parameter. In order to see whether this dependence is in accordance with one of the most popular theories of Liesegang patterning a numerical model based on Ostwald's supersaturation model has been solved in 2D and 3D. Results of these simulations are in a good agreement with the experimental observations. The time law was reformulated in order to incorporate the above mentioned geometrical effect.

© 2004 Elsevier B.V. All rights reserved.

1. Introduction

The first systematic investigations on quasi-periodic precipitate patterns were performed by their explorer Liesegang at the end of the 19th century [1–3]. In his experiments he applied an experimental setup with circular geometry. It means that he put a drop of concentrated solution of AgNO_3 onto a layer of gelatine, soaked with dilute solution of $\text{K}_2\text{Cr}_2\text{O}_7$.

Formation of Liesegang patterns can be characterized by several empirical regularities. The first and probably most important one is the so-called 'spacing law' which states that positions of the zones form a geometrical series. This means that denoting two adjacent zone positions by X_n and X_{n+1} , their relation will tend to a constant (spacing coefficient usually denoted by P) for n large enough [4,5]: $X_{n+1}/X_n = P$.

The second regularity or 'time law' describes the evolution of the zones. Using the previous notations and

denoting the time of appearance of the n th band by t_n we can find that $X_n = \beta_0 t_n^{1/2} + \gamma_0$, where β_0 and γ_0 are constants [5,7]. These two laws are valid for all geometries where the reaction front is closely planar.

The aim of the present paper is to investigate the evolution of the Liesegang pattern using a radial setup. As it is well known from the theory of chemical waves the curvature of the reaction front has a great impact on the velocity of the wave (curvature effect) [6]. Although Liesegang patterning is a heterogeneous process and in this respect it differs substantially from the autocatalytic systems, it is interesting to see whether such geometrical differences can affect the time law. In order to clarify this, we have carried out experiments with 2D radial arrangement varying the curvature of the boundary conditions. Numerical simulations in 2D and in 3D were also performed applying Ostwald's supersaturation theory.

2. Experimental

A gelatine gel disk swollen by $\text{K}_2\text{Cr}_2\text{O}_7$ solution with thickness of 1 mm was prepared. 1 g gelatine (Reanal)

* Corresponding author. Fax: +36 1 463 1896.

E-mail addresses: lagzi@vuk.chem.elte.hu (I. Lagzi), volfi@phyndi.fke.bme.hu (A. Volford), buki.andras@insilico.hu (A. Büki).

and 10 ml of 0.0036 M $K_2Cr_2O_7$ (Reanal) inner solution was heated to 65–75 °C and stirred for 20 min.

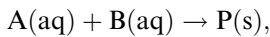
After complete dissolution of the gelling material 7.2 ml of the solution was poured into a Petri dish of diameter 9.6 cm. This container was held firmly horizontal to obtain uniformly 1 mm thick gel. The Petri dish was then covered and left undisturbed at room temperature (24 ± 2 °C) until completion of the gelation process. The next day a sheet of transparency film with a hole in the middle was put onto the outer surface of the gel.

Three different experiments were performed with hole radii 2, 3 and 6 mm.

The experiment was started by putting a few drops of 1.0 M $AgNO_3$ (Reanal) outer solution into the hole and set up the plastic $AgNO_3$ reservoir. The plastic reservoir is a 5 mm long tube with one end closed and with the same diameter as the hole in the foil. The closed end was leaky (by opening a hole with a pin) to supply $AgNO_3$ solution. The pattern formation was observed in transmitted light from neon lamp by a CCD camera (Panasonic WV-CP410.) connected to a computer. The pictures were taken every 5 min for 10 h.

3. The model

A numerical model, based on Ostwald's supersaturation theory [8], and formerly studied by Büki et al. [9,10] has been used to simulate the Liesegang patterning. A simple precipitation process can be described by the following chemical equation:



where $P(s)$ is the precipitate. Combining this reaction with the diffusive transport of the electrolytes the dynamical equations for such a system are the following:

$$\frac{\partial a}{\partial \tau} = D_a \nabla^2 a - \delta(ab, K, L), \quad (1a)$$

$$\frac{\partial b}{\partial \tau} = D_b \nabla^2 b - \delta(ab, K, L), \quad (1b)$$

$$\frac{\partial p}{\partial \tau} = \delta(ab, K, L), \quad (1c)$$

where a and b are the concentrations, D_a and D_b denote the diffusion coefficients of the species $A(aq)$ and $B(aq)$, respectively, while p is the amount of the precipitate. In our description all these quantities were dimensionless. τ is the dimensionless time, $\delta(ab, K, L)$ is the reaction term that describes the precipitation. According to the supersaturation theory the exact definition of this latter is the following:

if $p = 0$ there is no precipitate

$$\delta(ab, K, L) = \kappa \delta_p \Theta(ab - K),$$

if $p \neq 0$ there is some precipitate

$$\delta(ab, K, L) = \kappa \delta_p \Theta(ab - L),$$

where the formation of a bimer precipitate can be described by the following equation:

$$\delta_p = \frac{1}{2} \left[(a + b) - \left[(a + b)^2 - 4(ab - L) \right]^{1/2} \right],$$

where κ is the precipitation reaction rate constant, L is the solubility product, K denotes the nucleation product, function Θ is the Heaviside step function while δ_p is the amount of the reaction product.

For a radially symmetric experimental arrangement (feeding from a central point or a circle), the exact form of the above system of reaction-diffusion differential Eqs. (1a)–(1c) will be the following:

$$\frac{\partial a}{\partial \tau} = D_a \frac{\partial^2 a}{\partial r^2} + D_a \frac{N-1}{r} \frac{\partial a}{\partial r} - \delta(ab, K, L), \quad (2a)$$

$$\frac{\partial b}{\partial \tau} = D_b \frac{\partial^2 b}{\partial r^2} + D_b \frac{N-1}{r} \frac{\partial b}{\partial r} - \delta(ab, K, L), \quad (2b)$$

$$\frac{\partial p}{\partial \tau} = \delta(ab, K, L), \quad (2c)$$

Here r is the distance from the center and N is the number of spatial dimension. In our study, these equations were solved numerically using a second-order Runge–Kutta method with upwind approximation. Boundary conditions for all cases were the following:

$$a|_{r=r_0} = a_0 \quad \text{and} \quad \left. \frac{\partial b}{\partial r} \right|_{r=r_0} = \left. \frac{\partial a}{\partial r} \right|_{r=r_l-r_0} = \left. \frac{\partial b}{\partial r} \right|_{r=r_l-r_0} = 0,$$

where r_l-r_0 is the length of the reaction medium and r_0 is the radius of the hole.

Most of the input parameters were kept constant. Their values were chosen so that relatively large number of zones could evolve. The values of these fixed parameters were the following: $D_a = D_b = 0.4$, $K = 0.103$, $L = 0.1$, $\kappa = 10^3$ and $r_l-r_0 = 800$.

For the concentrations the following initial conditions were used:

$$a(0, r) = a_0 \Theta(r_0 - r) \\ b(0, r) = b_0 \Theta(r - r_0) \quad \text{and} \quad p(0, r) = 0,$$

where a_0 and b_0 are the initial concentration of the outer and inner electrolyte, respectively. Here we chose $b_0 = 1.0$, while a_0 and r_0 were varied in the simulations. The grid spacing and the time step were $\Delta r = 0.4$ and $\Delta \tau = 0.001$, respectively.

4. Results and discussion

Fig. 1 shows precipitate distributions for various hole radii. The density distribution functions were determined by a home made image processing software running on a Silicon Graphics workstation. The evolution curve (positions of the rings versus square root of time elapsed until their formation) is displayed in Fig. 2. According to the generally accepted ‘time law’ the evolution curve of patterns formed by planar fronts is linear. However, in our case where the fronts are circular, the positions of the rings can be accurately described by a second-order function. Moreover, the deviation from the linearity increases as the radius of the hole (r_0) decreases. Numerical simulations exhibit a similar trend (Fig. 3). In case of 1D simulation the evolution curve is linear. In a recent paper we have studied the effect of external electric field on 1D Liesegang patterning [11,12]. It was found that the distortion of the evolution curves can be described by a second order polynomial. From a purely mathematical point of view the governing equations of the two systems are very similar so we have applied the same type of approximation

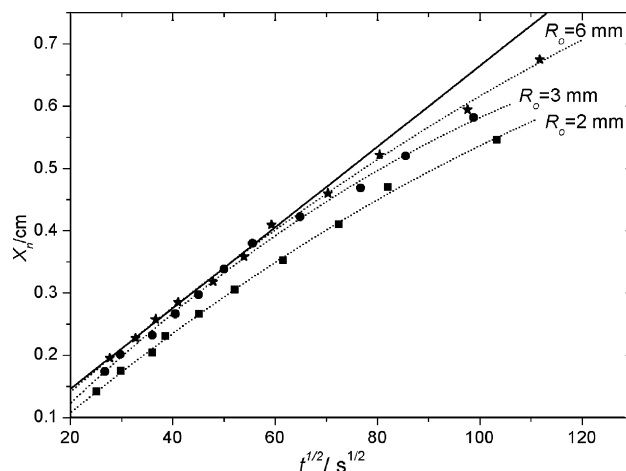


Fig. 2. Experimental evolution curves for different hole radii (R_0). The dotted lines are the fitted second-order curves. The solid line represents the fitted linear curve for first the seven points in case of $R_0 = 6$ mm.

$$X_n = \alpha(r_0, N)\tau + \beta(r_0, N)\tau_n^{1/2} + \gamma(r_0, N), \quad (3)$$

where $\alpha(r_0, N)$, $\beta(r_0, N)$ and $\gamma(r_0, N)$ are constants that depend on the radius and the spatial dimension. These parameters must satisfy the following constraints:

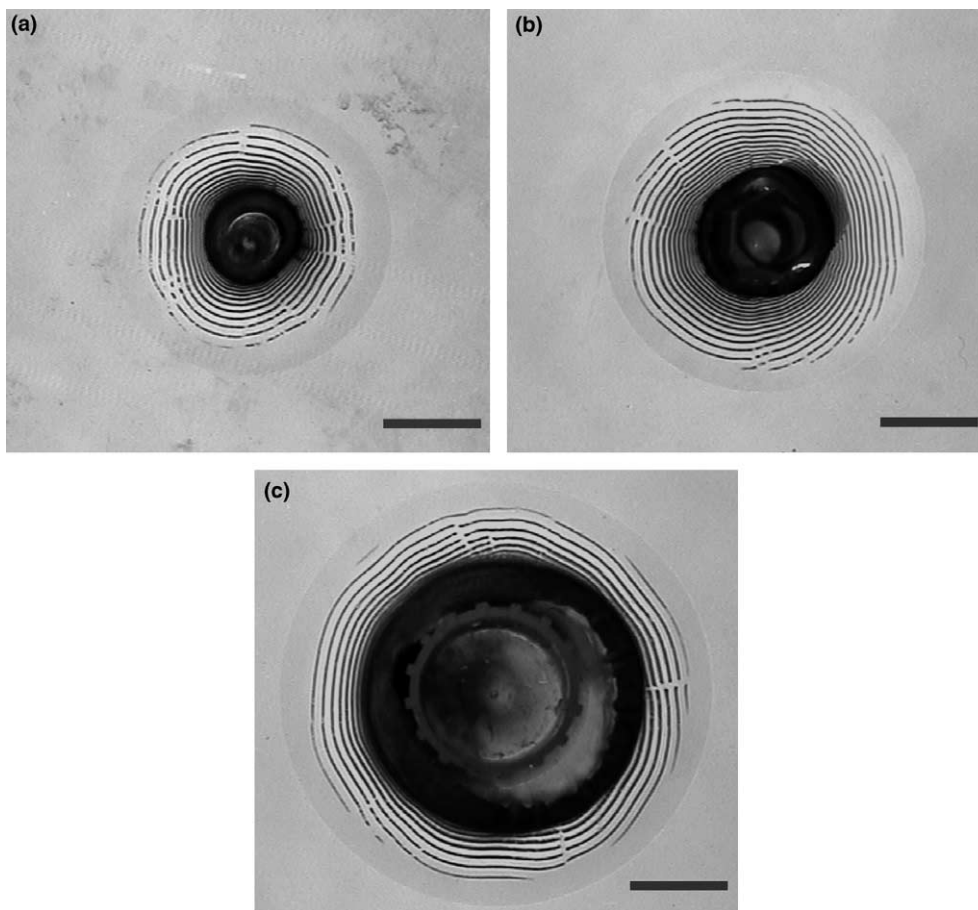


Fig. 1. The two dimensional precipitation patterns of AgNO_3 in gelatin gel ($[\text{AgNO}_3] = 1.0$ M and $[\text{K}_2\text{Cr}_2\text{O}_7] = 0.0036$ M) at 6.67 h after the start of the experiments: (a) $R_0 = 2$ mm; (b) $R_0 = 3$ mm; (c) $R_0 = 6$ mm. The scale bar is 1 cm.

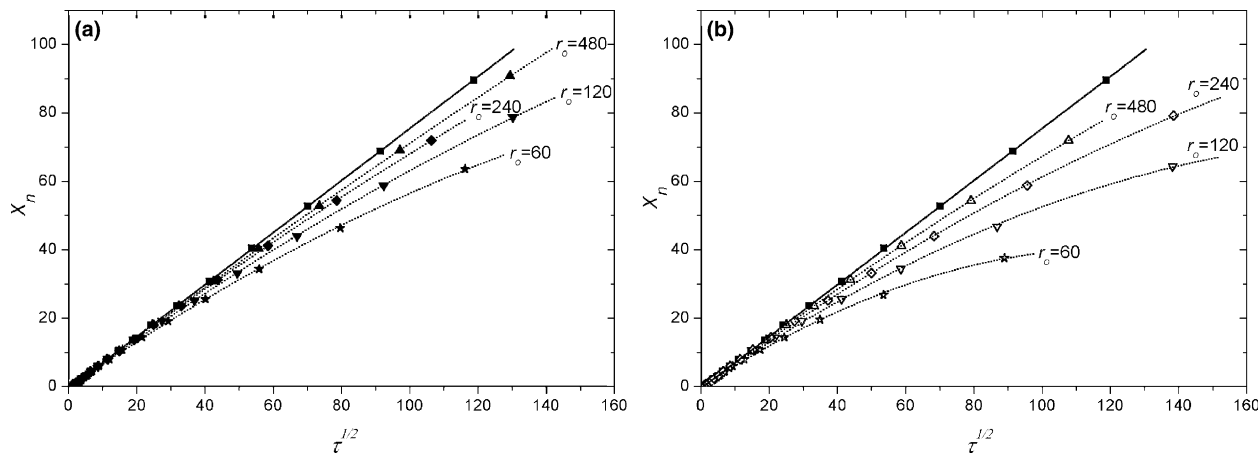


Fig. 3. Simulated evolution curves for different hole radii (r_0) in (a) 2D and (b) 3D at fixed initial concentration of the outer electrolyte ($a_0 = 1.0$). The dotted lines are the fitted second-order curves. The solid line represents the fitted linear curve in 1D simulation.

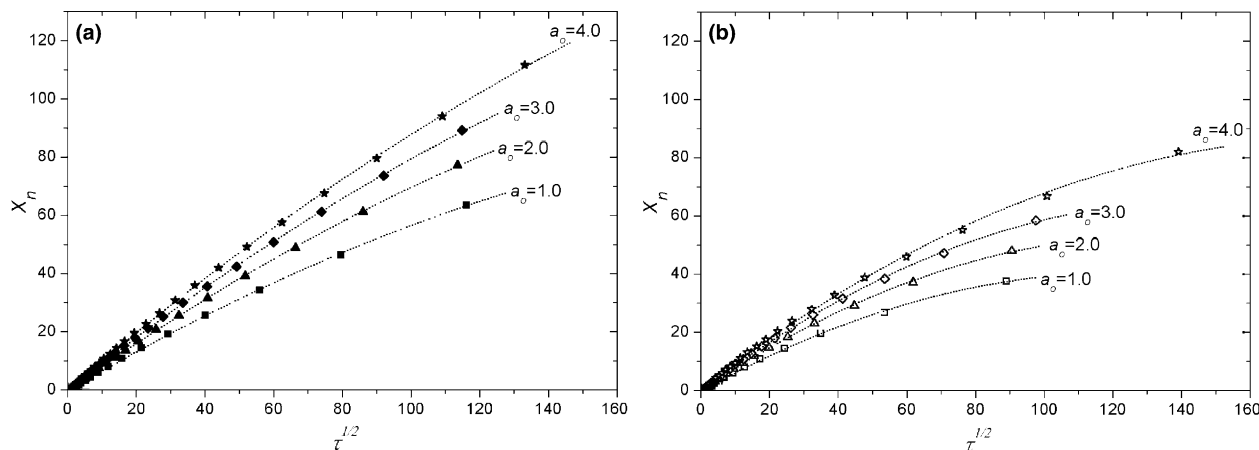


Fig. 4. Simulated evolution curves for different initial concentrations of the outer electrolyte (a_0) in (a) 2D and (b) 3D at fixed hole radius ($r_0 = 60$). The dotted lines are the fitted second-order curves.

$$\lim_{r_0 \rightarrow \infty} \alpha(r_0, N) = 0,$$

$$\lim_{r_0 \rightarrow \infty} \beta(r_0, N) = \beta_0,$$

$$\lim_{r_0 \rightarrow \infty} \gamma(r_0, N) = \gamma_0.$$

This former relation (3) is a more general form of the time law, which describe the evolution of the Liesegang pattern formation in all geometrical (planar, radial) conditions and spatial dimensions.

The decrease of r_0 causes a more and more pronounced deviation from the usual linear time law (Figs. 2 and 3). This effect becomes more conspicuous in 3D.

In case of a radial arrangement due to the initial and boundary conditions it is more convenient to describe the system in polar coordinates ((2a) and (2b)). The diffusion term consists of two parts, and the second, $\frac{N-1}{r}$ is usually not negligible. As the spatial dimension (N) increases this second term curvature effect becomes more expressed resulting in a slower evolution. The decrease

of radius (r_0) has the same impact. The initial condition has a direct impact on the beginning part of the pattern. At the same time the shift of the first precipitate zones changes the conditions of the whole evolution process.

We have investigated the effect of the outer electrolyte concentration on evolution of rings for fixed r_0 (Fig. 4). In both 2D and 3D cases similar trends can be observed. Increasing the concentration causes the rings to shift outward.

This effect has been observed in case of planar fronts where the front evolution line slope is increased. In our case the evolution curve becomes steeper in every point. Just like in case of planar fronts this is due to the higher mass flux.

5. Conclusions

Although Liesegang patterning is a relatively well studied phenomenon as to our best knowledge until

now the difference between planar and radial arrangements has not been investigated yet. At the same time it is physically plausible that the curvature of the initial and boundary conditions should have some impact on the evolution of such systems.

Recently several authors have studied patterning in 2D circular geometries [13–18] but their work was mainly focused on the mechanism of patterning.

In contrast during the work reported in this Letter, we have used one of the most simple mechanisms (supersaturation model) and studied the above mentioned geometrical effects.

2D experiments with radial arrangement were performed and the initial conditions (radius of the inner hole) were varied. Numerical simulations with similar initial and boundary conditions were performed in 2 and 3 dimensions. The effects found in the model calculations and in the real experiments show a good agreement.

We have concluded that the evolution of the radial patterns can be described by a second order function, which means that the usually applied time law suffers a weak distortion in these cases.

Acknowledgement

The authors thank Prof. Zoltán Noszticzius for his contribution to the experimental work. I.L. thanks for

the support of the OTKA grant D048673 and OMFB grant 00585/2003 (IKTA5-137) of the Hungarian Ministry of Education. A.V. thanks for the support of Békésy György stipendium.

References

- [1] R.E. Liesegang, *Naturwiss. Wochenschr.* 11 (1896) 353.
- [2] S. Kai, S.C. Müller, *Sci. Form* 1 (1985) 9.
- [3] S.C. Müller, J. Ross, *J. Phys. Chem. A* 107 (2003) 7997.
- [4] K. Jablczynski, *Bull. Soc. Chim. Fr.* 33 (1923) 1592.
- [5] J. George, G. Varghese, *Chem. Phys. Lett.* 362 (2002) 8.
- [6] J.J. Tyson, J.P. Keener, *Physica D* 32 (1988) 327.
- [7] H.W. Morse, G.W. Pierce, *Proc. Am. Acad. Arts Sci.* 38 (1903) 625.
- [8] W. Ostwald, *Kolloid Zeit.* 36 (1925) 380.
- [9] A. Büki, E. Kárpáti-Smidróczki, M. Zrínyi, *J. Chem. Phys.* 103 (1995) 10387.
- [10] A. Büki, E. Kárpáti-Smidróczki, M. Zrínyi, *J. Chem. Phys.* 375 (1995) 357.
- [11] I. Lagzi, *Phys. Chem. Chem. Phys.* 4 (2002) 1268.
- [12] I. Lagzi, F. Izsák, *Phys. Chem. Chem. Phys.* 5 (2003) 4144.
- [13] H.-J. Krug, H. Brandtstädter, *J. Phys. Chem. A* 103 (1999) 7811.
- [14] R. Sultan, S. Panjarian, *Physica D* 157 (2001) 241.
- [15] I. Das, S. Chand, A. Pushkarna, *J. Phys. Chem.* 93 (1989) 7435.
- [16] I. Das, A. Pushkarna, A. Bhattacharjee, *J. Phys. Chem.* 95 (1991) 3866.
- [17] L. Zeiri, O. Younes, S. Efrima, M. Deutsch, *Phys. Rev. Lett.* 79 (1997) 4685.
- [18] U. Sydow, P.J. Plath, *Ber. Bunsen. Phys. Chem.* 102 (1998) 1683.